ELSEVIER

Journal of Alloys and Compounds 404–406 (2005) 144–149

Journal of ALLOYS AND COMPOUNDS

www.elsevier.com/locate/jallcom

Ce-valence state and hydrogen-induced volume effects in Ce-based intermetallic compounds and their hydrides

M. Stange[a], V. Paul-Boncour[b], M. Latroche[b], A. Percheron-Guégan[b], O. Isnard[c], V.A. Yartys[a,*]

[a] *Institute for Energy Technology, P.O. Box 40, Kjeller N 2027, Norway*
[b] *Laboratoire de Chimie Metallurgique des Terres Rares, GLVT, CNRS, 2 rue H. Dunant, F-94320 Thiais, France*
[c] *Laboratoire de Cristallographie du CNRS, associe a l'Universite Jousepfh Fourier et a l'INPG, BP166X, F-38042 Grenoble, Cedex 9, France*

Received 6 September 2004; accepted 20 September 2004
Available online 2 August 2005

Abstract

An average Ce-valence state (v) of two types of Ce-containing intermetallic compounds, equiatomic CeNiX (X =Al, Ga, Sn) and CeM_3 (M =Ni, Co, Mn), and their hydrides was estimated from X-ray absorption spectroscopy (XAS) and analysed in parallel with hydrogen-induced volume changes on hydrogenation. The largest valence states in the initial compounds were found in CeM_3 ($v = 3.32 - 3.36$) followed by $CeNiAl_{1-x}Ga_x$($v = 3.25 - 3.27$). This contrasts to CeNiSn, which is close to a pure trivalent state ($v = 3.07$). On hydrogenation, a conversion from mixed-valent $CeNiAl_{1-x}Ga_x$, $x = 0.5$, 1, to pure Ce^{III} hydrides takes place ($\Delta V/V = 19.6 - 20.0\%$). In $CeNiSnD_z$ ($z = 1$, 1.8, $\Delta V/V = 3.0$, 8.0%) the changes in the valence state towards Ce^{III} are very small. The situation for the CeM_3-hydrides is complex. For $CeNi_3D_{2.8}$, $CeNi_{2.75}Mn_{0.25}D_{3.4}$ and $CeCo_3D_{3.4}$ ($\Delta V/V = 24 - 32\%$) where rather similar electronic properties can be expected, a decrease in the contribution of Ce^{IV} for $CeNi_3D_3$ and $CeNi_{2.75}Mn_{0.25}D_{3.4}$ ($v = 3.18$ and 3.12, respectively) contrasts to the behaviour of $CeCo_3D_{3.4}$ where the hydrogen induced valence change is very small ($v = 3.32$).

Keywords: Hydrogen storage materials; Intermetallics; EXAFS; X-ray diffraction; Synchrotron radiation

1. Introduction

The physical properties of metals and intermetallic compounds are significantly altered upon hydrogenation. Magnetism, conductivity, optical and mechanical properties are dramatically modified when hydrogen atoms are accommodated in the metal lattice.

Hydrogen induced volume changes vary significantly from system to system. Although an average volume expansion of 2.5–3.0 $Å^3$/at.H is often observed for intermetallic hydrides, both negative and positive deviations from this value are frequently observed due to modifications of the electronic structures and the crystal structure of the metal and hydrogen sublattices.

Ce-containing intermetallic compounds form a very specific group of materials. Volumes much smaller than anticipated are often characteristic for cerium intermetallics compared to isostructural intermetallics of the other rare earth metals. This volume contraction is related to an intermediate valence state characterised by a significant contribution of the $4f^0$ (Ce^{IV}; Pearson metallic radius for $Ce^{3.6}$ 1.715 Å) compared to $4f^1$ (Ce^{III}; Pearson metallic radius for $Ce^{3.1}$ 1.825 Å [1]) electronic configurations.

Magnetisation and electrical resistivity measurements show that hydrogenation leads to a reduction in the cerium valence state from intermediate values to a pure trivalent state in several intermetallic cerium compounds including CeNiAl [2] and CeNiGa [3]. Such transitions are often accompanied by a significant volume increase.

In this contribution the cerium valence states of selected Ce-intermetallics and hydrides were probed and re-

* Corresponding author. Tel.: +47 63 80 64 53; fax: +47 63 81 29 05.
E-mail address: volodymyr.yartys@ife.no (V.A. Yartys).

0925-8388/$ – see front matter © 2005 Elsevier B.V. All rights reserved.
doi:10.1016/j.jallcom.2004.09.088

lated to changes of volume upon hydrogenation. Two groups of compounds having equiatomic CeNiX (X =Al, Ga, Sn) stoichiometry and CeM_3 (M =Mn, Co, Ni) compositions were studied by powder X-ray (synchrotron) diffraction and X-ray absorption spectroscopy (XAS). The sample choice was made on the background of differences in volume behaviour upon hydrogenation; CeNiX (X =Al, Ga) and CeM_3 (M =Mn, Co, Ni) show a significant volume increase ($\Delta V/V \sim$ 20–30%) whereas the volume expansion upon hydrogenation for CeNiSn is significantly smaller ($\Delta V/V <$ 10%).

CeNiAl and CeNiGa crystallize with the hexagonal ZrNiAl-type of structure at room temperature (space group $P\bar{6}2m$) [3,4] while upon hydrogenation, the symmetry transforms into the AlB_2-type structure (space group $P6/mmm$) [2,3]. CeNiSn crystallizes in the orthorhombic TiNiSi-type of structure (space group $Pnma$) [5]. Hydrogenation takes place in two steps forming a lower hydride, CeNiSnH with the NdNiSnD-type structure (space group $Pna2_1$) [6] and a higher hydride $CeNiSnH_{1.8}$ with the hexagonal $LaNiSnD_2$-type structure (space group $P6_3/mmc$) [7]. The structures of $CeNi_3$ and $CeCo_3$ are, respectively, hexagonal (space group $P6_3/mmc$) and trigonal (space group $R\bar{3}m$), consisting of alternating slabs of CeM_2 and CeM_5 stacking along the c-axis [8,9]. The hydrogenation takes place in the CeM_2 slabs and results in an unusually high anisotropic expansion, ~30% expansion along the [0 0 1] direction in $CeNi_3H_{2.8}$ [10] leading to an orthorhombic symmetry lowering (space group $Pmcn$) [10].

2. Experimental

CeNiAl, CeNiGa, $CeNiGa_{0.5}Al_{0.5}$, CeNiSn, $CeNi_3$, $CeNi_{2.75}Mn_{0.25}$ and $CeCo_3$ were prepared by arc melting of starting elements of at least 99.9% purity. They were thereafter annealed at 600 °C (CeNiX) or 900 °C (CeM_3) for 3 weeks and quenched into ice. Sample purity was tested by X-ray diffraction (Siemens D5000 diffractometer, Cu Kα_1 radiation, Bragg Bretano geometry) and except for traces of CeO_2 and an unidentified impurity phase (<5 wt.%) in CeNiSn and <5 wt.% $CeNi_2$ in $CeNi_{2.75}Mn_{0.25}$, the alloys were single-phase materials.

The samples were activated in secondary vacuum at 400 °C for 1–2 h before deuteration. The deuterides were synthesised with deuterium gas having a purity of 99.8%. Deuteration of the $CeNiGa_{1-x}Al_x$ alloys was performed at room temperature under a deuterium pressure of approximately 4 bar. CeNiSnD was deuterated at 5 bar at 390 °C [6] while the high deuteride $CeNiSnD_{1.8}$ was heated to 250 °C under a deuterium pressure of 40 bar and cooled to room temperature to achieve a complete saturation of the sample with deuterium [7]. The CeM_3 samples were deuterated at room temperature at pressures of approximately 2 bar. After deuteration all samples were kept and handled in an argon-filled glove box.

Synchrotron X-ray diffraction data for selected samples were collected at the Swiss Norwegian Beamlines (SNBL), ESRF, Grenoble, $\lambda = 0.5000$ Å. For all other samples, powder X-ray diffraction (PXD) data were collected with a Siemens D5000 diffractometer in flat-plate transmission geometry using monochromatic Cu Kα_1 radiation from a Ge-monochromator. Silicon was used as internal standard and for calibration. Rietveld analyses were carried out using the GSAS software [11].

CeL_{III} XAS experiments were performed at the XAFS II station at LURE (Orsay, France) using a double Si(3 1 1) monochromator. The higher harmonics were eliminated by adjusting the parallelism between the two Si-crystals. The two ionization chambers were filled with air. The CeL_{III} edge was calibrated against a Cr-foil. The samples were ground in an agate mortar, sieved through a 15 μ mesh to provide small particle size and then spread evenly on a kapton tape placed on a small Al-disc with a 0.5 cm×2 cm hole. The samples were sealed with another layer of tape to prevent contact with air during the measurements. The spectra were background subtracted and normalized to the height of the absorption edge. The data analysis was done by using a convolution of a lorentzian, gaussian and arctan funtion for the white lines for Ce^{III} and Ce^{IV}. The arctan function describes the electron transition from 2p to the continuum states and the Lorentzian function describes the transition from 2p to the unoccupied 5d states.

3. Results

3.1. Crystal structures

Unit-cell parameters of CeNiGa, $CeNiGa_{0.5}Al_{0.5}$, CeNiSn, $CeNi_3$, $CeNi_{2.75}Mn_{0.25}$ and $CeCo_3$ alloys and their corresponding deuterides as determined from Rietveld refinements of X-ray diffraction patterns, are listed in Table 1. The collected crystal structure data for CeNiX (X =Al, Ga, $Ga_{0.5}Al_{0.5}$, Sn) intermetallics and hydrides (X =Ga, $Ga_{0.5}Al_{0.5}$, Sn) were found to be in good agreement with reference material. The volume expansion of CeNiX (X =Al, Ga, $Ga_{0.5}Al_{0.5}$) upon hydrogenation is significant, $\Delta V/V \sim$ 20.0% giving 4.6 Å^3/D for $GeNiGaD_{2.4(1)}$ and 3.7 Å^3/D for $CeNiGa_{0.5}Al_{0.5}D_{3.0(2)}$. The deuterium content in CeNiGa is significantly higher than reported previously ($CeNiGaH_{1.1}$ [3]). We note that assuming H/CeNiGa= 1.1 gives a volume expansion of 10.0 Å^3/at.H which drastically exceeds the average values for the metal hydrides, 2.5–3.0 Å^3/at.H. This supports a suggestion that actual H-storage capacity of CeNiGa is higher as observed in the present work. Published hydrogen content for CeNiAl varies between $CeNiAlH_{1.93}$ [2] (7.0 Å^3/H) and $CeNiAlH_{2.85}$ [12]. Using similar argument as discussed for CeNiGa, it can be expected that H-content in CeNiAl-based hydride should exceed 2 at.H/f.u.

An interesting feature discovered during our refinements of the powder diffraction data for the CeNiSn-based samples is a mutual substitution of Ni and Sn found for CeNiSn and $CeNiSnD_2$ (approximately 13% substitution of both Ni (by Sn) and Sn (by Ni) in both compounds) which kept the overall stoichiometry of the metal lattice unchanged, CeNiSn). These data differ from the previously published results where a complete ordering of Sn and Ni was stated. The detailed presentation of our refinements of the crystal structures will be published in a forthcoming paper [13].

Despite we have observed some indications of the mutual substitution of Ni and Ga in $CeNiAl_{1-x}Ga_x$ (negative displacement factors for Ni), a possible Ni/Ga(Al) site mixing in $CeNiAl_{1-x}Ga_x$could not be determined conclusively from the available X-ray diffraction data. A complementary powder neutron diffraction study is required to resolve this problem.

Unit-cell dimensions of CeM_3 (M =Ni, Co, Mn) alloys and hydrides are listed in Table 1. Collected data are in good agreement with previously published results for $CeNi_3D_{2.8}$ [6]; partial substitution of Ni by Mn to form $CeNi_{2.75}Mn_{0.25}$ does not affect the mechanism of hydrogenation: the same type of orthorhombic deformation of the hexagonal unit cells takes place with a sole expansion along the *c*-axis. However, the crystallinity of the deuteride deteriorates during the doping of the sample with Mn. In a quite complex structure of $CeCo_3D_{3.4}$ the hydrogen-induced expansion proceeds along [0 0 1] and is accompanied by a volume expansion of ∼32%.

3.2. XAS

The normalized Ce L_{III}-XAS data of the $CeNiGa_{1-x}Al_x$, $x = 0$ and 0.5, and the deuterides $CeNiGaD_{2.4}$ and $CeNiGa_{0.5}Al_{0.5}D_{3.0}$ are shown in Fig. 1. We note that the H storage behaviour of the mixed Ga + Al sample is similar to the observed in this work behaviour of CeNiGa (2.4 at.D/f.u.) and the reference data for $CeNiAlH_{2.85}$ [12]. For the intermetallic phases both the two white lines assigned to Ce^{III} and Ce^{IV} (corresponding to two electron transitions from the $2p_{3/2}$ core level to the $4f^1(5d6s)^3$ and $4f^0(5d6s)^4$ empty states, respectively) confirm the mixed valence state for cerium. The fractional part of Ce^{III} and Ce^{IV} can be determined with the convolution method. The valence state of cerium appears to be roughly independent of x; CeNiGa $v = 3.25(1)$, $CeNiGa_{0.5}Al_{0.5}$ and CeNiAl, $v = 3.27(1)$ (Ce^{III} at 5725 eV and Ce^{IV} at 5734 eV in all cases). Upon hydrogenation a localisation of the 4f(Ce) states gives a pure trivalent state, $v = 3.00(1)$, for $CeNiGaD_{2.4}$ (this work), $CeNiGa_{0.5}Al_{0.5}D_{3.0}$ (this work) and $CeNiAlH_{1.93}$ [3].

Cerium in the CeNiSn alloy is almost trivalent however a small contribution from Ce^{IV} cannot be ruled out (Fig. 2). A strict quantification of the small amounts of the Ce^{IV} channel is difficult, however a course estimate will be $v = 3.07$, i.e., significantly lower than for the $CeNiGa_{1-x}Al_x$ alloys. For the CeNiSn–D system the XAS data for the two hydrides, CeNiSnD and $CeNiSnD_{1.8}$ the cerium state is purely trivalent.

The highest cerium valence state is found (Fig. 3) in $CeCo_3$ ($v = 3.36(2)$), $CeNi_3$ and $CeNi_{2.75}Mn_{0.25}$ ($v = 3.32(2)$). For $CeNi_3D_{2.8}$ and $CeCo_3D_{3.4}$ ($\Delta V/V = 27.5$–32%), where similar electronic properties can be expected, the decrease in the contribution of the Ce^{IV} channel for $CeNi_3H_{2.8}$ ($v = 3.18(2)$) contrasts to the behaviour of $CeCo_3D_{3.4}$ where the hydrogen induced valence change is very small ($v = 3.31(2)$). While the substitution of Mn into the Ni sites did not influence the cerium valence in the two alloys, a lower contribution of the Ce^{IV} channel is found in $CeNi_{2.75}Mn_{0.25}D_{3.4}$ ($v = 3.12(2)$). The volume expansion upon hydrogenation is slightly smaller for $CeNi_{2.75}Mn_{0.25}$

Table 1
Unit cell data[a] for the initial intermetallic compounds and their hydrides, the relative volume expansion on hydrogenation and Ce valence state (*v*Ce)

Composition	Space group	Structure type	*a*(Å)	*b* (Å)	*c* (Å)	*V* (Å^3)	$\Delta V/V$(%)	*v*Ce	Ref.
CeNiAl	$P\bar{6}2m$	ZrNiAl	6.9760(5)		4.0187(5)	169.36(1)	–	3.27	[4]
$CeNiAlH_{1.93}$	$P6/mmm$	AlB_2	4.27(1)		4.43(1)	69.95(5)	20.0	3.00	[2]
CeNiGa	$P\bar{6}2m$	ZrNiAl	6.9507(1)		3.9789(1)	166.472(4)	–	3.25	This work
$CeNiGaD_{2.4}$	$P6/mmm$	AlB_2	4.2587(4)		4.2390(7)	66.581(5)	20.0	3.00	This work
$CeNiGa_{0.5}Al_{0.5}$[a]	$P\bar{6}2m$	ZrNiAl	6.9748(8)		4.0241(5)	169.54(4)	–	3.27	This work
$CeNiGa_{0.5}Al_{0.5}D_{3.0}$[a]	$P6/mmm$	AlB_2	4.253(1)		4.314(3)	67.59(3)	19.6	3.00	This work
CeNiSn[a]	$Pnma$	TiNiSi	7.5391(1)	4.5973(1)	7.6301(1)	264.45(1)	–	3.07	This work
CeNiSnD	$Pna2_1$	NdNiSnD	7.2788(5)	8.4974(7)	4.4028(4)	272.32(2)	2.98	3.00	This work
$CeNiSnD_{1.8}$[a]	$P6_3/mmc$	ZrBeSi	4.39210(1)		8.54493(5)	142.753(1)	8.04	3.00	This work
CeNiIn	$P\bar{6}2m$	ZrNiAl	7.522		3.974	194.7	–	>3.0	[19]
$CeNiInH_{1.8}$	$P\bar{6}2m$	ZrNiAl	7.291		4.624	213.0	9.41	3.00	[20]
CeNiGe	$Pnma$	TiNiSi	7.2469(5)	4.3083(3)	7.2379(6)	226.00(8)		>3.0	[15]
$CeNiGeH_{1.8}$	$P6_3/mmc$	ZrBeSi	4.190(1)		8.293(2)	126.08(3)	11.6	c	[15]
$CeNi_3$	$P6_3/mmc$	$CeNi_3$	4.97004(4)	4.9700(1)	16.5165(2)	353.321(1)	–	3.32	This work
$CeNi_3D_{2.8}$	$Pmcn$	$CeNi_3D_{2.8}$	4.8748(3)	8.5590(5)	21.590(2)	900.81	27.5	3.18	[10]
$CeCo_3$	$R\bar{3}m$	$PuNi_3$	4.9573(1)		24.7396(9)	526.52(2)		3.36	This work
$CeCo_3D_{3.4}$[a]	Orthorhombic	$PuNi_3$ related	∼4.92	∼8.82	∼ 32.72	∼ 1390	∼ 32	3.31	[10]
$CeNi_{2.75}Mn_{0.25}$[a]	$P6_3/mmc$	$CeNi_3$	5.01588(4)		16.5241(2)	360.033(5)		3.32	This work
$CeNi_{2.75}Mn_{0.25}D_{3.4}$[a,b]	Orthorhombic		∼4.86	∼8.54	∼ 21.47	∼ 892	∼ 24	3.12	This work

[a] SR-XRD data.
[b] The phase is of low crystallinity but the structure resembles that of $CeNi_3D_{2.8}$.

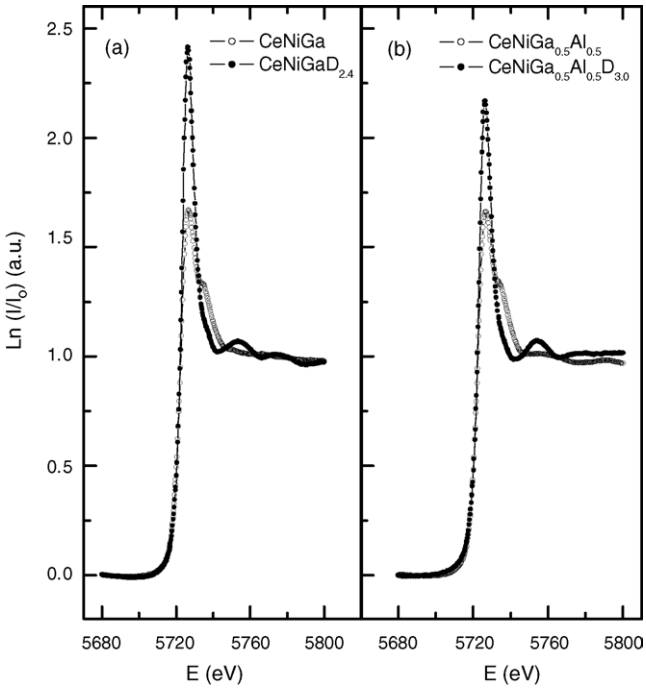

Fig. 1. Experimental Ce L_{III} XAS spectra of CeNiGa and $CeNiGa_{0.5}Al_{0.5}$ and their hydrides $CeNiGaD_{2.4}$ and $CeNiGa_{0.5}Al_{0.5}D_{3.0}$.

($\Delta V/V = \sim 24\%$) than for $CeNi_3$ and $CeCo_3$. The position of the white lines are Ce^{III}: 5725 eV and Ce^{IV}: 5734 eV in all cases. The fit to the Ce L_{III}-edge data of $CeNi_3D_{2.8}$ is shown in Fig. 4 as an example of the quality typically obtained in Ce L_{III} XAS valence refinements.

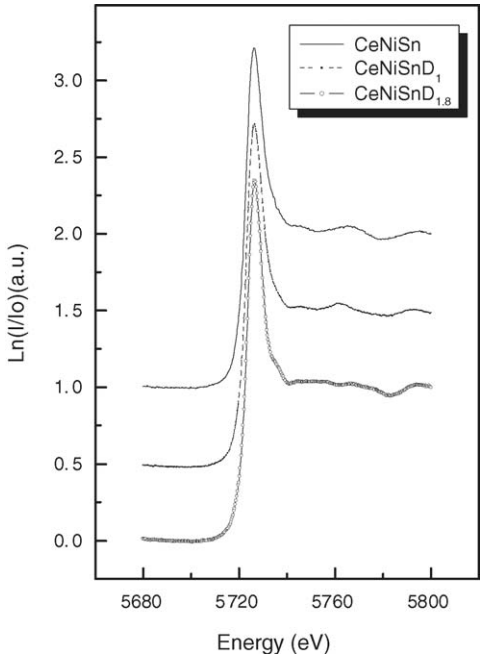

Fig. 2. Experimental data of the Ce L_{III} edge of CeNiSn, CeNiSnD and $CeNiSnD_{1.8}$.

4. Discussion

The presently studied hydrides of equiatomic intermetallic compounds show that the volume expansion creates in all cases very expanded H-occupied Ce_3Ni tetrahedra with large radii ranging from 0.58 (CeNiSnD) to 0.72 Å ($CeNiSnD_{1.8}$). A significant difference in the expansion behaviour between CeNiSn and $CeNiAl_{1-x}Ga_x$ is related to two features: (a) the size of Ce_3Ni in the initial CeNiSn is originally large, 0.62 Å, so no further expansion is required at all to accommodate H atoms; this contrasts to the Al- and Ga-containing alloys where the Ce_3Ni site is rather small at the beginning, 0.35 Å; (b) the valence of Ce in CeNiSn change very little on hydrogenation, and does not give any contribution to the expansion behaviour on H absorption.

Because of the large differences in Sn-radii compared to Al and Ga ($r_{Sn} = 1.623$ Å versus $r_{Al} = 1.432$ Å;$r_{Ga} = 1.411$ Å [1]), the above result could be easily explained by the significantly larger size of Sn-based unit cells giving a less densely packed structure allowing for a higher Ce^{III} character in CeNiSn and a larger Ce_3Ni tetrahedra. However, a comparison with the magnetic behaviour of two other mixed cerium valence state intermetallics, CeNiIn [14] and CeNiGe [15], shows that their electronic structure behaviours do not correlate with the crystallographic changes upon hydrogenation. In $CeNiInH_{1.8}$ [14] pure trivalent cerium is observed while the hydrogen occupied tetrahedral Ce_3Ni site is relatively small, 0.53 Å. In contrast, a mixed valence state of Ce is reported for $CeNiGeH_{1.6}$ [15] despite a presence of much larger (0.60 Å) Ce_3Ni tetrahedra.

Thus, it is clear that the volume effects upon hydrogenation of CeNi*X* (Al, Ga, In, Ge, Sn) are not closely related to the valence state of Ce. Instead, their electronic structure seems to be influenced by the behaviour of the *X* element and hydrogen storage capacity of the materials.

The volume expansion of CeM_3 upon hydrogenation is large ($\Delta V/V > 24\%$) although the hydrides, as the initial intermetallics, still have significant contribution of Ce^{IV}. A comparison of the Ce L_{III} XAS spectra for all CeM_3 samples and hydrides are given in Fig. 3. The $CeNi_3$-type intermetallic structure contains alternation of $CeNi_2$ and $CeNi_5$ layers. Crystal structure studies [10] have established that there is a huge expansion of the $CeNi_2$ layers (63.1%) contrary to the $CeNi_5$ layer which does not contain hydrogen at all and slightly contracts on hydrogenation (−2.8%). Thus, a Ce^{IV} contribution is still anticipated for the hydride phase assuming unchanged valence state of the $CeNi_5$ layer. From this assumption the valence state of cerium in $CeNi_2$ ($v2$) can be calculated to be 3.11 ($0.33 \times 3.32 + 0.67 \times v2 = 3.18$) in $CeNi_3D_{2.8}$ An important conclusion from this is that even extremely high anisotropic expansion of the $CeNi_2$ layers does not convert Ce to a pure Ce^{III} valence state. The valence changes of Ce upon hydrogenation of CeM_3 closely resembles that of CeY_2Ni_9 [16] where the valence change from $v = 3.36(6)$ to 3.19(1) upon hydrogenation to $CeY_2Ni_9D_{8.1}$.

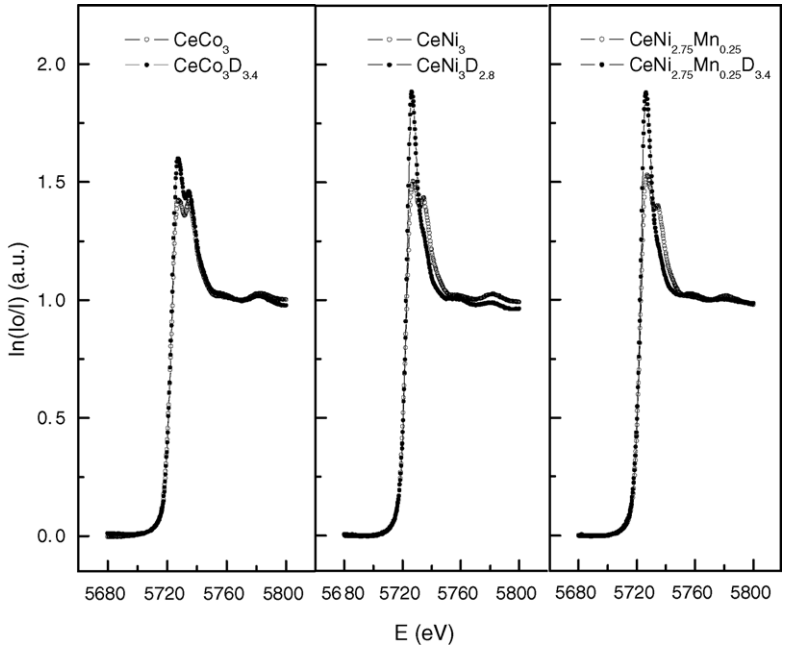

Fig. 3. Experimental Ce L_{III} XAS spectra of $CeCo_3$, $CeNi_3$ and $CeNi_{2.75}Mn_{0.25}$ and their hydrides.

The situation is slightly different for $CeNi_{2.75}Mn_{0.25}D_{3.4}$, as the change of cerium valence in the $Ce(Ni,Mn)_2$ layer is more significant than in pure $CeNi_3$ and can be calculated to be 3.02 ($v2$) in $CeNi_{2.75}Mn_{0.25}D_{3.4}$.

Finally, the behaviour of $CeCo_3$ is even more complex. The crystallographic changes observed on hydrogenation, sole pronounced expansion along [0 0 1] (32%) is even more significant compared to $CeNi_3D_{2.8}$ (30.7%). However, for the compound of Co preliminary refinements show that both $CeCo_5$ and $CeCo_2$ layers are hydrogenated which corresponds to the behaviour of the binary intermetallic compounds $CeCo_2$ [17] and $CeCo_5$ [18]. However, this probable hydrogen absorption by both layers does not have a significant effect on the average valence state which only slightly decreases from 3.36 in $CeCo_3$ to 3.31 in $CeCo_3H_{3.4}$.

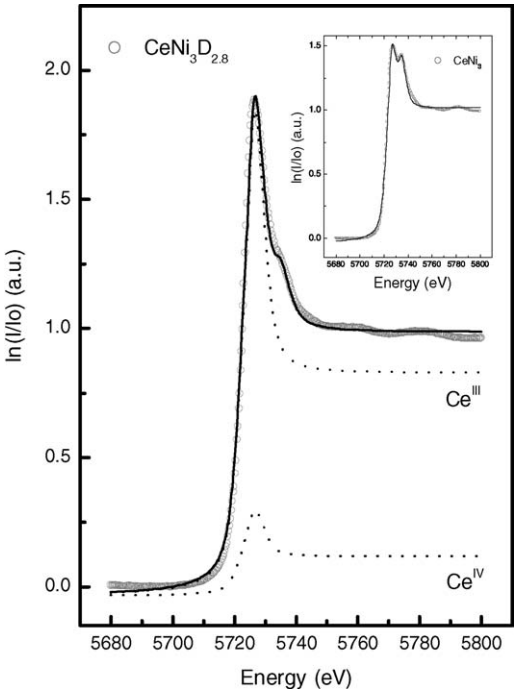

Fig. 4. L_{III} edge of cerium for the deuteride $CeNi_3D_{2.8}$ where Ce^{III} and Ce^{IV} is observed. The full line corresponds to the refinements assuming Ce^{III} (at 5725 eV) and Ce^{IV} (at 5734 eV).

In conclusion, big volume changes on hydrogenation do not necessarily correspond to the Ce valence change in Ce-intermetallics. The electronic structure of the studied Ce-containing materials appears to be much more complex and does not allow applying simple straightforward correlations of the valence and volume changes during hydrogen absorption.

Acknowledgements

The beamline responsible, R. Cortes, at the XAFS 2 station at LURE, Orsay, France and the beamline team at the Swiss-Norwegian Beamlines, ESRF, Grenoble, France are gratefully acknowledged. This study has received a support from the Norwegian Research Council.

References

[1] W.P. Pearson, The Crystal Chemistry and Physics of Metals and Alloys, Wiley/Interscience, New York, 1972.

[2] J.-L. Bobet, B. Chevalier, B. Darriet, M. Nakhl, F. Weill, J. Etourneau, J. Alloys Compd. 317–318 (2001) 67.
[3] B. Chevalier, J.-L. Bobet, E. Gaudin, M. Pasturel, J. Etourneau, J. Solid State Chem. 168 (2002) 28.
[4] A.E. Dwight, H.M. Mueller, R.A. Conner Jr., J.W. Downey, H. Knatt, Trans. Metall. AIME 242 (1968) 2075.
[5] R.V. Skolozdra, O.E. Koretskaya, K. Yu, Gorelenko, Inorg. Mater. 20 (1984) 520.
[6] V.A. Yartys, B. Ouladdiaf, O.Yu. Khyzhun, K.H.J. Buschow, J. Alloys Compd. 359 (2003) 62.
[7] B. Chevalier, J.-L. Bobet, M. Pasturel, E. Gaudin, F. Weill, R. Decourt, J. Etourneau, Chem. Mater. 15 (2003) 2181.
[8] D.T. Cromer, C.E. Olsen, Acta Crystallogr. 12 (1959) 689.
[9] V.A. Yartys, V.V. Burnasheva, K.N. Semenenko, Adv. Chem. 52 (1983) 529.
[10] V.A. Yartys, O. Isnard, A.B. Riabov, L.G. Akselrud, J. Alloys Compd. 356 (2003) 109.
[11] A.C. Larson, R.B. von Dreele, General Structure Analysis System (GSAS). LANSCE, MS-H 805, 1994.
[12] B. Bandyopadhyay, K. Ghoshray, A. Ghoshray, N. Chatterjee, Phys. Rev. B 46 (1992) 2912.
[13] M. Stange, V.A. Yartys, in preparation.
[14] B. Chevalier, M.L. Kahn, J-L. Bobet, M. Pasturel, J. Etourneau, J. Phys. Condens. Matter 14 (2002) 365.
[15] B. Chevalier, M. Pasturel, J.-L. Bobet, F. Weill, R. Decourt, J. Etourneau, J. Solid State Chem. 177 (2004) 752.
[16] M. Latroche, V. Poul-Boncour, A. Percheron-Guégan, J. Solid State Chem. 177 (2004) 2542.
[17] R.A. Sirotina, K.N. Semenenko, W. Burnasheva, Zhurnal Obshchei Khimii 61 (1991) 2638.
[18] F.A. Kuijpers, B.O. Loopstra, J. Phys. Chem. Solids 35 (1974) 301.
[19] P. Villars, L.D. Calvert, Pearson's Handbook of Crystallographic Data for Intermetallic Phases, American Society for Metals, Ohio, 1985 p. V1–3.
[20] I.I. Bulyk, V.A. Yartys, R.V. Denys, Ya.M. Kalychak, I.R. Harris, J. Alloys Compd. 284 (1999) 256.